Phenol photocatalytic degradation over Fe-TiO$_2$ materials synthesized by different methods

D. Hurtado-Jimenez (iD) ; E. Arriola-Villaseñor (iD) , E. Berrio-Mesa (iD) , J. A. Hernandez-Maldonado (iD) , T. A. Zepeda (iD) , G. M. Hincapié-Triviño (iD) , R. Barrera-Zapata (iD) , A. N. Ardila-Arias (iD)

Abstract—The photocatalytic activity and stability of 3% Fe-TiO$_2$ materials synthesized by incipient wet impregnation (% Fe-TiO$_2$-DP25) and sol-gel (3% Fe-TiO$_2$-sol-gel) were studied using the phenol degradation as test reaction. The effects of various operation parameters including photocatalyst concentration, solution pH and initial H$_2$O$_2$ concentration on phenol degradation were also investigated. The higher phenol degradation was achieved using 26 mg of photocatalyst, H$_2$O$_2$ initial concentration of 600 mg/l and initial pH of 3.0 with both materials. It was found that 3% Fe-TiO$_2$-DP25 enhanced activity, achieving a 99% phenol degradation, in comparison with 70% phenol degradation with the 3% Fe-TiO$_2$-sol-gel. Notwithstanding, the material prepared by incipient wet impregnation method, evidenced leaching of iron ions from the material surface. Therefore, this catalyst is not suitable for the phenol degradation for environmental and economic reasons. The catalyst prepared by the sol-gel method did not show iron leaching during the reaction and maintain its catalytic activity after several reuses.

Index Terms— Fe photocatalyst, impregnation wetness incipient, photocatalytic stability, Sol-gel Method,

Resumen—Se estudió la actividad fotocatalítica y estabilidad de materiales 3% Fe/TiO$_2$ sintetizados por impregnación húmeda incipiente (3% Fe/TiO$_2$-DP25) y sol-gel (3% Fe/TiO$_2$-sol-gel), usando fenol como molécula modelo. Se evaluó el efecto de parámetros de operación como concentración de fotocatalizador, H$_2$O$_2$ y pH de la solución. Los mayores porcentajes de degradación de fenol con ambos materiales se lograron utilizando 26 mg de fotocatalizador y 600 Mg/Ll de H$_2$O$_2$ a un pH de 3.0. El mejor porcentaje de degradación de fenol (99%) se obtuvo usando el catalizador 3% Fe/TiO$_2$-DP25, en comparación a un 70% con el material 3% Fe/TiO$_2$-sol-gel. No obstante, el material preparado por impregnación húmeda incipiente fue inestable evidenciando lixiviación de hierro. Por lo tanto, este catalizador no es adecuado para la degradación de fenol debido a razones ambientales y económicas. El catalizador preparado por sol-gel no mostró lixiviación de hierro durante la reacción y mantuvo su actividad y estabilidad catalítica después de varios reúsos.

Palabras claves— estabilidad fotocatalítica, fotocatalizadores de hierro; impregnación húmeda incipiente, método sol-gel.

I. INTRODUCTION

ADVANCED oxidation processes (AOPs) are suitable techniques in the degradation of organic pollutants since they can mineralize the pollutants completely into carbon dioxide and water. AOPs involving hydrogen peroxide, ozone and/or Fenton reagents, with or without a source of UV radiation have been used for the photo-oxidation of organic pollutants. These processes involve the generation of reactive hydroxyl free radicals that are potent enough to oxidize many organic contaminants. Moreover, such techniques are considered to be of low-cost, because the moderate temperature and pressure conditions required for complete mineralizing of pollutants in relatively short times [1]. Among those AOPs, processes using Fenton type reagent are relatively cheap and easy to operate and maintain.

Photo-Fenton techniques involve homogeneous systems widely used in the treatment of industrial wastewaters [2]. However, one of the drawbacks of the reaction is the draining of the ferrous catalyst and the hydrolysis of iron ions (limited pH range) [3, 4]. In addition, the homogeneous Fenton process requires up to 50-80 mg/L Fe in solution, which exceeds the limits set by EU directives that allow a maximum of 2 mg/L Fe in treated water to be discharged directly into the environment

[5, 6]. Heterogeneous catalysis systems could solve part of these problems providing an easy separation and recovery of the catalyst from the treated wastewater, since most are noncorrosive and are environmentally friendly.

Up to date, TiO_2 has been the heterogeneous photocatalyst most widely studied because of its high photocatalytic activity, photochemical stability, non-toxicity and low cost. However, the efficiency of using TiO_2 is limited by its relatively large band gap energy (3.2 eV), matching to the wavelength of 370 nm where only 3-5% of solar energy can be used [7]. In addition, this material has a high degree of recombination of photogenerated species which limit the efficiency of the photocatalytic processes [8]. TiO_2 doping with transition metals has been employed for solving this disadvantage [9]. In this sense, Fe^{3+} is widely used since it originates a localized narrow band above the valence band of titanium which makes the catalyst sensitive to visible light absorption [10]. Iron-doped TiO_2 has gained attention due to the fact that Fe^{3+} radius (78.5 pm) is similar to that of Ti^{4+} (74.5 pm) resulting in easier insertion of Fe^{3+} into the crystal structure of TiO_2 [11]. Thus, the heterogeneous photo-Fenton catalysts could solve the problem of removing Fe from the reaction system at the end of the process [12], nevertheless the iron stability on the photocatalyst will depend on the reaction conditions and/or on the catalyst synthesis method.

The sol–gel method is one of the most widely used techniques to prepare TiO_2-based photocatalyst. The incorporation of metal ions (dopants) in the sol allows the ions to have direct interaction with the polycondensation of titanium alkoxide during the sol-gel process, and the lattice of TiO_2 can be doped with metal ions. It presents advantages such as the use of relatively simple equipment, the possibility of using different substrates, and the ability to control the microstructure, homogeneity and density of materials [13]. On the other hand, incipient wet impregnation method is frequently used due to its simple execution and low waste streams.

In this context, in the present work it was studied the stability and activity of Fe-doped TiO_2 photocatalysts prepared by incipient wet impregnation and sol-gel methods. These photocatalysts were used for the degradation of phenol as test reaction. Moreover, the effects of initial pH, H_2O_2 concentration, and photocatalyst concentration on the reaction system were also studied. Phenol degradation was selected as test reaction because phenol is considered to be one of the important organic pollutants discharged into the environment causing significant damage and threat to the ecosystem in water bodies and human health [14, 15]. It is moreover classified as a teratogenic and carcinogenic agent. Thus, phenol is listed in water hazard class 2 in several countries. Biodegradability is only 90% in surface waters after seven days, and the aquatic toxicity of phenol (LC50) is 12 mg/L [5, 16, 17].

II. MATERIALS AND METHODS

A. Synthesis of catalysts

The 3%Fe-TiO_2-DP25 photocatalysts were synthesized by wet-impregnation method on commercial TiO_2 (Degussa, P-25 powder) with the required amount of $FeSO_4.7H_2O$ dissolved in water (5 mL water/g TiO_2). Solids were dried at 100 °C for 1 h and calcined at 600 °C during 4 h under static air. The 3%Fe-TiO_2-sol-gel photocatalysts were synthesized by sol-gel method, mixing 9.2 mL of titanium butoxide and 23 mL of butanol at room temperature. After adjusting the pH to 9 with NH_4OH, 0.3 g of $FeSO_4.7H_2O$ were dissolved in 11.5 mL deionized water, which was added dropwise. The gel was stirred under reflux for 23 h at 55 °C. Finally, the temperature was raised to 70 °C with constant stirring during 6 h. The solvent was removed from gels in a rotary evaporator at 70 °C for 2 h. Solids were dried and calcined as mentioned above. For comparison purposes in the catalytic tests, undoped TiO_2 materials were prepared in a similar manner by omitting the $FeSO_4.7H_2O$ precursor.

B. Characterization techniques

Loading of Fe in the fresh catalysts and in the catalyst after reaction was verified by Atomic Absorption Spectroscopy (AAS) (Agilent, model Spectra AA-240FS). In all cases the AAS value for fresh catalysts matched the nominal content within 3%. The crystalline phases were determined from X-ray powder diffraction patterns collected in air at room temperature with a Bruker D-8 Advance diffractometer (Bragg-Brentano θ-θ geometry, Cu Kα radiation, a Ni 0.5% Cu-Kβ filter in the secondary beam, and a one-dimensional position-sensitive silicon strip detector (Bruker, Lynxeye)). The diffraction intensity was measured in the 15-70° 2θ range using a 0.02°/min 2θ step rate. The identification of the phases was made with the help of the Joint Committee on Powder Diffraction Standards files (JCPDS), and the data was processed using Jade 6.0 software. Crystallite sizes were calculated from the line broadening of the main XRD peaks by using the Scherrer equation.

UV-vis spectra of the samples were recorded on a Varian Cary 5E UV-VIS-NIR Spectrophotometer with a Praying Mantis Diffuse Reflection Accessory. Band-gaps values were calculated from the corresponding Kubelka-Munk functions (F(R∞)), which are proportional to the absorption of radiation, by plotting (F(R∞) × hυ)1/2 against hυ. The surface areas of the materials were determined by the BET method from N_2 isotherms measured at 75.2 K with a Quantachrome Autosorb Automated instrument. The pore diameter and volume distributions were determined using the BJH method (PD BJH and PV BJH, respectively). The point of zero charge (pzc) of the samples was determined by the method of mass titration, which involves finding the asymptotic value of the pH of an oxide/water slurry as the oxide mass content is increased. Different amounts of powders were added to water (typical values of oxide/water by weight were 20, 40, 60, 80 y 100 mg) and the resulting pH values were measured after 24 h of

equilibration. The pH values of the point of zero charge (pHPZC) were estimated from potentiometric titration.

The X-ray photoelectron spectra of the samples were recorded using a SPECS® spectrometer with a PHOIBOS® 150 WAL hemispherical energy analyzer with angular resolution (< 0.5 degrees), equipped with a XR 50 X-Ray Al/Mg-x-ray and μ-FOCUS 500 X-ray monochromator (Al excitation line) sources. The binding energies (BE) were referenced to the C 1s peak (284.5 eV) to account for the charging effects. The areas of the peaks were computed after fitting of the experimental spectra to Gaussian/Lorentzian curves and removal of the background (Shirley function). Surface atomic ratios were calculated from the peak area ratios normalized by the corresponding atomic sensitivity factors.

C. Photocatalytic activity

The photocatalytic tests were performed in cylindrical glass reactors (diameter: 6.5 cm, depth: 4.5 cm) containing 200 mL of a 50 mg/L phenol solution under UV artificial irradiation by 3 hours. A cabin Centricol (with the following effective working area: width 74 cm, length 34 cm, height 35 cm) equipped with four 15 W Tecnolite fluorescent tubes with emission spectrum from 300 to 400 nm (maximum around 365 nm) as UV source in photocatalytic experiments. According to photo-catalytic phenol degradation studies available in the literature [2, 3, 6], all of the experiments were carried out at constant temperature (~ 30 °C) and a magnetic stirring speed of 260 rpm. In order to favor the adsorption-desorption equilibrium, prior to irradiation the suspension was magnetically stirred for 10 min in absence of light.

The final samples were analyzed by HPLC, using a Shimadzu Prominence CTO-20A chromatograph, which was equipped with a diode array DAD detector and a C18 reverse column (3 μm, 4.6 mm × 50 mm). The HPLC analysis was carried out using water acidified with phosphoric acid (pH 3.0)/methanol (95:5) as mobile phase, a flow rate of 0.8 mL/min and 40 °C.

Photolysis tests of phenol under UV light and in absence of photocatalyst were carried out. Under the experimental conditions used in this work, substrate photolysis was not observed in any case. In order to evaluate the effect of operative conditions during the photodegradation of phenol the photocatalytic measurements were evaluated following a three-level factorial experimental design (3x3) (Table 1) with 3%Fe-TiO₂-DP25 and 3%Fe-TiO₂-sol-gel photocatalysts. The factorial design and ANOVA statistical tests were carried out with Statgraphics Centurion XV (Stat Point Technologies, Inc.). In this work, the maximization of the phenol removal was selected as the optimization goal of the heterogeneous process whereas the initial pH, the amount of photocatalyst and the hydrogen peroxide concentrations were selected as independent variables. Maximun and minimum levels for the evaluated factors were selected according to literature reports regarding phenol degradation studies [2, 3, 6].

TABLE I
FACTORS AND LEVELS OF THE EXPERIMENTAL DESIGN

	Factors	Levels		
		i	j	k
α	H_2O_2 concentration (mg/L)	200	400	600
β	Initial pH	3.0	5.0	7.0
γ	Photocatalyst concentration (mg/L)	32.5	65	130

III. RESULTS AND DISCUSSION

A. Photocatalyst characterization

Fig. 1 shows the XRD patterns of pure TiO_2 (DP25 and sol-gel), 3%Fe-TiO_2-DP25 and 3%Fe-TiO_2-sol-gel photocatalysts. Peaks marked as ● and ◊ correspond to the anatase and rutile phases of TiO_2, respectively. The rutile peak intensities decrease with the presence of Fe [5, 18, 13].

The 3%Fe-TiO_2-DP25 revealed some peaks related to isolated iron-bearing phases, which correspond to hematite phase (α-Fe_2O_3), with diffraction peaks appearing at $2\theta = 24.1$, 33.1, 35.7 and 49.5. In contrast, 3%Fe-TiO_2-sol-gel reveals only an extra weak peak at $2\theta = 30.6°$, which corresponds to the same hematite phase (α-Fe_2O_3).

This may due to the synthesis method, which favored that Fe^{2+} ions replace some of the T^{i4+} ions into the TiO_2 lattice, because the radii of Ti^{4+} and Fe^{2+} ions are very similar [7, 13, 19].
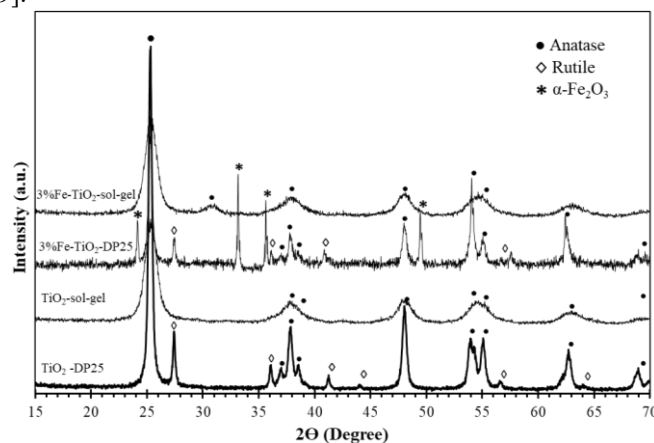
Fig. 1. XRD patterns of photocatalysts. Peaks marked as ● and ◊ correspond to the anatase and rutile phases of TiO_2, respectively.

The crystallite sizes of TiO_2-DP25, TiO_2-sol-gel, 3%Fe-TiO_2-DP25 and 3%Fe-TiO_2-sol-gel are 35.0, 26.6, 32.6 and 10.8 nm, respectively (Table 2), which is determined from the full-width at half maximum of the anatase (101) peak by the Scherrer's formula. In comparison with the pure TiO_2-DP25 and TiO_2-sol-gel supports, the doped catalysts, both materials are of similar sizes.

TABLE II
PHOTOCATALYST PHYSICOCHEMICAL PROPERTIES

Property	Photocatalyst			
	TiO_2-DP25	TiO_2-sol-gel	3%Fe/TiO_2-DP25	3%Fe/TiO_2-sol-gel

Band gap (eV)	3.25	3.20	2.90	2.50
Isoelectric point	6.7	6.1	2.8	2.6
S_{BET} (m²/g)	49.2	66.5	47.2	62.9
PV BJH (cm³/g)	1.34	0.91	0.62	0.26
PD BJH (nm)	5.7	7.8	3.9	6.5
Crystallite size (nm)	35.0	26.6	32.6	10.8

The textural properties of all materials are also shown in Table 2. Porosity parameters are also slightly affected by the presence of iron ions incorporated into the TiO_2 lattice. The decrease in surface area after doping may be caused by a decrease in the regularity of the mesoporous structure of TiO_2. However, whether the activity of a photocatalyst can be directly related to the catalyst surface area is still a debating issue since photocatalytic reactions are believed to proceed only on the illuminated surface. Therefore, between the prepared materials the separation efficiency of photo-generated hole/electron pairs could become one of the main factors to control the photocatalytic activity [11].

Thus, the band gap energies calculated by lineal regression of the plot $(F(R\infty) \times h\upsilon)1/2$ against $h\upsilon$ (Table 2) show that the band gap energy of the 3%Fe-TiO_2-DP25 and 3%Fe-TiO_2-sol-gel are lower than the obtained for both undoped materials, which may be one of the reasons of the improvement in the photocatalytic activity. The isoelectric point of all materials are shown in Table 2. Presence of Fe ions in titania crystal lattice caused shifts in isoelectric point, this can be attributed to different phenomena as changes in cation coordination, structural charge, ion exchange capacity, among others.

UV-vis results are shown in Fig. 2. The wide absorption band between 200 and 400 nm is due to the electron transitions of the valence band to the conduction band of pure TiO_2 (DP25 and sol-gel). When compared UV spectra of undoped materials with 3%Fe-TiO_2-DP25 and 3%Fe-TiO_2-sol-gel, differences are
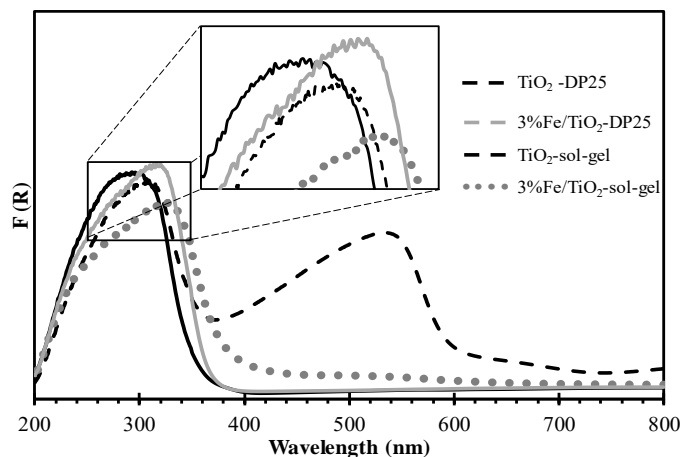

Fig. 2. UV-Vis spectra recorded for the photocatalysts

observed in this band. This is attributed to the charge transfer transition between the d-electrons of Fe and the conduction

band of the TiO_2, which indicates that Fe is present as a substitutional dopant inside the TiO_2 particles, decreasing the electromagnetic radiation required for its excitation [13]. The improvement of the absorption in the visible light region (400-600 nm) for the Fe-doped TiO_2 photocatalysts compared to that of the undoped TiO_2, indicates their potential to absorb visible light and improve photocatalytic activities under visible light illumination [13, 19, 20].

The Fe 2p and Ti 2p core-level spectra of TiO_2 sol-gel and 3%Fe-TiO_2-sol-gel are shown in Fig. 3 and Fig. 4, respectively. Furthermore, the binding energy (BE) values of the Ti $2p_{3/2}$, Fe $2p_{3/2}$ core levels and surface Fe/Ti atomic ratio are summarized in Table 3.

TABLE III
BINDING ENERGIES (EV) OF CORE LEVELS AND SURFACE ATOMIC RATIOS

Sample	Ti $2p_{3/2}$	Fe$2p_{3/2}$	Fe/Ti atomic
3%Fe-TiO_2-DP25	458.4	710.8 (74%) 709.1 (26%)	0.0115
3%Fe-TiO_2-sol-gel	458.4 (81%) 459.7 (19%)	710.4	0.0052

All samples showed an intensive Ti $2p_{3/2}$ peak at 458.4 eV, and it is associated with the presence of Ti^{4+} ions [21]. An additional Ti $2p_{3/2}$ peak at 459.7 eV was observed in the TiO_2-sol-gel and 3%Fe-TiO_2-sol-gel photocatalysts, which corresponds to tetrahedrally coordinated titanium, this is typically observed in titanium oxides synthesized by sol-gel
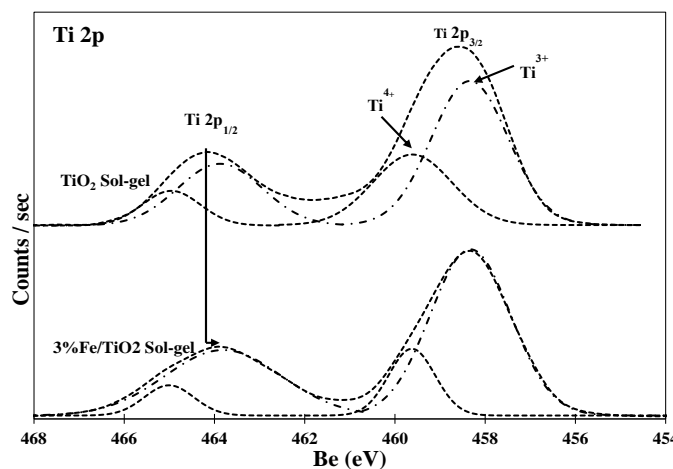
Fig. 3. XPS spectra of Ti 2p core levels for the photocatalysts

method [22, 23].

For the case of the materials prepared by sol-gel method, the Ti $2p_{3/2}$ energy band of the Fe-doped photocatalyst shift to a lower binding energy compared with TiO_2-sol-gel, indicating a higher electron density of the Ti atoms in the %Fe-TiO_2-sol-gel photocatalyst. This is because the electrons of Fe^{3+} transfer toTi^{4+}, which results in the increasing in the outer electron cloud densities of Ti ions and lower the binding energies of the Fe-doped photocatalyst [23].

The deconvolution of the Fe peak show that the Fe $2p_{3/2}$ and

Scientia et Technica Año XXIV, Vol. 24, No. 03, septiembre de 2019. Universidad Tecnológica de Pereira.

527

Fe $2p_{1/2}$ presents two main peaks: Fe^{2+} at 710.8 eV and Fe^{3+} at 718.1 together with their satellites [23].

The $3\%Fe/TiO_2$-DP25 photocatalyst showed a BE for Fe $2p_{3/2}$ peak at 710.8 eV, this signal is characteristic of Fe^{3+} species. In the $3\%Fe/TiO_2$-sol-gel sample the BE position of this band showed a lower BE value (710.4 eV). This displacement could indicate that occurs some enrichment in the electronic environmental of the surface iron cations [24, 25]. It can be assumed that strong interactions between Ti and Fe ions occurs since the Fe and Ti oxides were synthesized simultaneously by sol-gel method, which favored that Fe^{3+} ions substitute Ti^{4+} ions in the TiO_2 lattice, as observed in DRS-UV-vis results.

Then, it is expected that a transfer transition from conduction band of the TiO_2 toward the d-electrons of Fe occurs. Additionally, in the $3\%Fe/TiO_2$-DP25 catalyst a minor BE
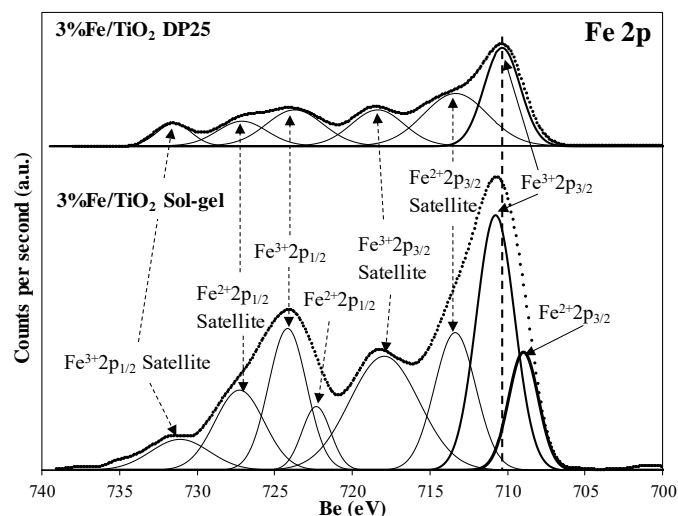

Fig. 4. XPS spectra of Fe 2p core levels for the photocatalysts.

signal was observed at 709.1 eV, which is characteristic to the presence of Fe^{2+} species. The presence of this signal could be related whit the presence of bigger α-Fe_2O_3 particles. The surface Fe/Ti atomic ratio has resulted 2.2 times higher in the $3\%Fe/TiO_2$-DP25 catalyst in comparison with Fe catalyst synthesized by sol-gel method, this result reveals an important degree of surface segregation of the iron in consistency with the presence of the band at 535 nm in the UV-vis spectra. Thus it can be assumed that in the $3\%Fe/TiO_2$-sol-gel sample, some fraction of Fe ions are located into of Ti oxide framework.

B. Photocatalytic performance

Prior to the photocatalytic degradation experiments, photodegradation of phenol on the pure TiO_2-DP25 and TiO_2-sol-gel was investigated. The results showed a low phenol photodegradation for both the TiO_2-DP25 (15% removal) and TiO_2-sol-gel (28% removal) after 3 hours of UV irradiation. The phenol degradation was only 26% and 35% for the TiO_2-DP25 and TiO_2-sol-gel, respectively when 200 mg/L of H_2O_2 was added at initial pH of 3.0, which is higher than that in the presence of either pure TiO_2-DP25 or TiO_2-sol-gel.

ANOVA results during photocatalytic process for the $3\%Fe$-TiO_2-DP25 and $3\%Fe$-TiO_2-sol-gel photocatalysts are presented in Table 4. ANOVA table decomposes the variability of the percentage degradation of phenol into contributions due to studied factors. With both materials the complete P-values are lower than 0.05, which means that the studied factors have a statistically significant effect on percentage degradation of phenol at the 95.0% confidence level.

The dosage of photocatalyst is an important parameter in degradation processes. In this study, different concentrations of photocatalysts were tested. The Fig. 5 shows the degradation results of phenol at different pH and initial H_2O_2 concentration with several dosages for $3\%Fe$-TiO_2-DP25 and $3\%Fe$-TiO_2-sol-gel photocatalysts, in all cases within 3 hours of UV irradiation.

TABLE IV
ANOVA RESULTS FOR THE EXPERIMENTAL RESPONSE OF PHENOL REMOVAL % AT DIFFERENT LEVELS OVER $3\%Fe$-TiO_2-DP25 AND $3\%Fe$-TiO_2-SOL-GEL

Source	DF	SS	MS	F	P
$3\%Fe$-TiO_2-DP25					
α:H_2O_2 initial	2	6563.8	3281.9	1304.3	0.0000
β: initial pH	2	857.38	428.69	170.37	0.0000
γ:Catalyst(mg)	2	2730.4	1365.2	542.54	0.0000
$\gamma\beta$	4	450.39	112.60	44.750	0.0000
$\gamma\alpha$	4	633.01	158.25	6.2900	0.0010
$\beta\gamma$	4	650.38	162.60	6.4600	0.0009
$\gamma\beta\alpha$	8	120.24	150.30	5.9700	0.0002
Residual Error	27	67.940	25.163		
Total (Corrected)	53	10918			
$3\%Fe$-TiO_2-sol-gel					
α:H_2O_2 initial	2	1854.4	927.18	590.98	0.0000
β: initial pH	2	3939.3	1969.6	1255.4	0.0000
γ:Catalyst(mg)	2	12445	6222.6	3966.3	0.0000
$\gamma\beta$	4	656.56	164.14	10.460	0.0000
$\gamma\alpha$	4	517.13	129.28	82.400	0.0000
$\beta\gamma$	4	145.72	364.29	23.220	0.0000
$\gamma\beta\alpha$	8	165.49	206.86	13.190	0.0000
Residual Error	27	42.360	156.89		
Total (Corrected)	53	19175			

DF: degree of freedom, SS: Sequential sum of square, MS : Mean squared

For both materials, the results show that when photocatalyst concentration increases from 32.5 to 65 mg/L, phenol degradation slightly increases; however, further increase in photocatalyst concentration to 130 mg/L results in a significant increase in phenol degradation. The same tendency was observed for the different pH values evaluated. For the case of H_2O_2, phenol degradation increased with the increase in its concentration. Moreover, the photocatalysis show no significant differences at pH 3.0 and pH 5.0, but it decreased when the pH was 7.0, which could be attributed to the formation of non-active, poorly soluble iron species at pH = 7.0.

The best operation conditions found for the phenol degradation over $3\%Fe$-TiO_2-DP25 (99%) and $3\%Fe$-TiO_2-sol-gel (70%) were the same (H_2O_2 concentration of 600 mg/L and initial pH of 3.0). The higher photoactivity of $3\%Fe$-TiO_2-DP25 in comparison with $3\%Fe$-TiO_2-sol-gel would be explained by Fe^{3+} ions leached from the iron oxide-impregnated samples, which act as a homogeneous photocatalytic system for the

phenol photodegradation. This phenomenon suggests the possibility that species originated from iron lixiviates can participate in the reaction mechanism [23]. Nevertheless, it is difficult to differentiate between homogeneous and heterogeneous photocatalytic effects.

It is well known that the complete mineralization of phenol occurs through the formation of several reaction intermediates, such as p-benzoquinone (yellow color), o-benzoquinone (red color), and hydroquinone (color-less) and/or maleic and other carboxylic acids, some of them being even more toxic than phenol itself, and the mixed solution of all intermediate compounds revealed a brown color [5, 23]. The final reaction solutions used with 3%Fe-TiO2-DP25 photocatalyst showed a certain brownish color, which is in agreement with the observations performed [23], and may point to the presence of p-benzoquinone and/or o-benzoquinone intermediates. However, this may also be due to the species originated from iron lixiviates. Therefore, the mineralization of phenol was thus evaluated through total organic carbon (TOC) measurements. The results evidence that phenol was not fully mineralized over 3%Fe-TiO2-DP25, while almost 100% TOC, total
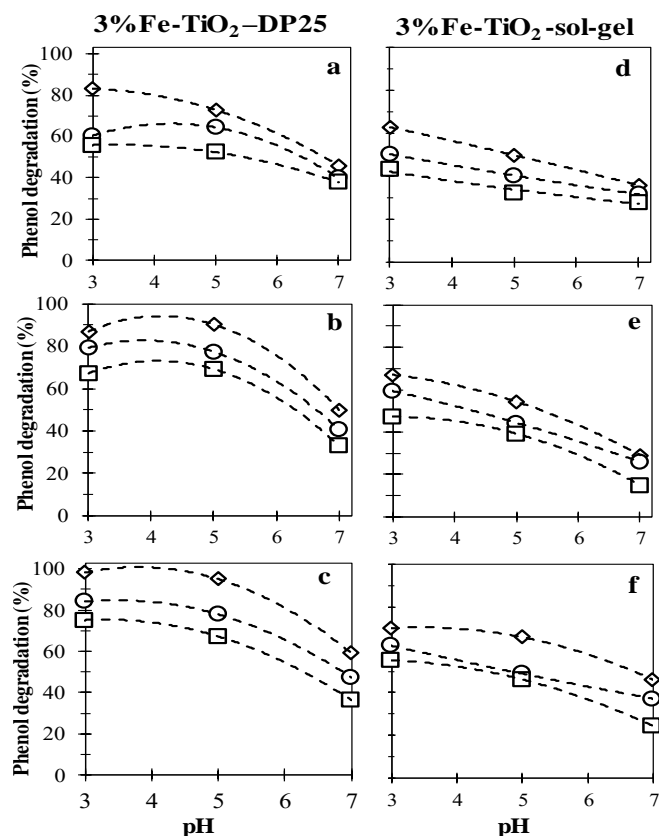

Fig. 5. Photocatalytic activity at different photocatalyst concentration (a and d are 32.5 mg/L, b and e are 65 mg/L and c and f are 130 mg/L), different solution pH and different initial H_2O_2 (◊ 600 mg/L, o 400 mg/L and □ 200 mg/L) over both 3%Fe-TiO2-sol-gel and 3%Fe-TiO2-DP25 materials.

mineralization of phenol was obtained after 3 hours of photodegradation in the presence of the 3%Fe-TiO2-sol-gel (Fig. 6).

C. Photocatalyst stability

In order to determine the stability of the photocatalysts, the 3%Fe-TiO2-DP25 and the 3%Fe-TiO2-sol-gel materials were reused after recovering from the reaction system by simple filtering and water rinsing. When the 3%Fe-TiO2-DP25 was reused by first time, there was a significant decrease in percentage of phenol removal; it decreased from 99% to 55% after 3 h of UV irradiation. In addition, when the same material was reused by second time, the percentage of phenol degradation decreased slightly up to 45%, but then it was stabilized. Moreover, XRD characterization of 3%Fe-TiO2-DP25 after reaction showed the intensities of α-Fe2O3 diffraction peaks were decreased. In addition, AAS analysis of the reaction media showed that about 19.4% of Fe leached to the reaction solution (Table 5). These results suggest that the underlying deactivation mechanism involves the dissolution of some of α-Fe2O3 nanoparticles. On the other hand, the variation in phenol degradation during the first and second reuses appears to be caused by the initial loss of Fe from the fresh photocatalyst to the reaction solution. However, leaching of Fe decreased during further uses until Fe in the photocatalyst reached a stable residual level closer to 2.2 wt %. The fact that Fe was lixiviated from the photocatalysts is a proof that the photodegradation

Fig. 6. Final aliquots of the reaction solutions for the best reaction conditions.

occurs on the surface of the semiconductor and that it is also catalyzed by dissolved Fe cations (Photo-Fenton process).

When the 3%Fe-TiO2-sol-gel photocatalyst was reused once, the activity decreased slightly (from 70% to 68%), and then it remained approximately constant during further reuses. This material did not exhibit Fe leaching during the phenol photodegradation.

TABLE V
FE CONTENT FOR FRESH AND REUSED PHOTOCATALYSTS

Photocatalyst	Fe load wt %			Fe leaching %	
	Fresh	Used once	Used twice	Used once	Used twice
3%Fe-TiO2-DP25	3.1	2.5	2.2	19.4	12
3%Fe-TiO2-sol-gel	2.8	2.8	2.8	0.0	0.0

IV. CONCLUSIONS

It was shown that 3%Fe-TiO$_2$-sol-gel prepared by sol-gel method, exhibited higher performance photocatalytic than 3%Fe-TiO$_2$-DP25 synthesized by incipient wet impregnation method and supports TiO$_2$. Moreover, the 3%Fe-TiO$_2$-sol-gel photocatalyst exhibited better stability than 3%Fe-TiO$_2$-DP25. The stability of the 3%Fe-TiO$_2$-DP25 photocatalyst by recycled experiments revealed that the percentage degradation of phenol in the second cycle, is around 45%. The activity for the 3%Fe-TiO$_2$-sol-gel showed a slight decrease with the recycling times (68%); thus, the 3%Fe-TiO$_2$-sol-gel material prepared by sol-gel method has good stability in performance reaction.

REFERENCES

[1] A. M. Abdullah, N. J. Al-Thani, K. Tawbi,. and H. Al-kandari, "Carbon/nitrogen-doped TiO$_2$: New synthesis route, characterization and application for phenol degradation," Arab. J. Chem, vol. 9, No. 2, pp. 229–237, 2016, DOI: 10.1016/j.arabjc.2015.04.027.

[2] M. Dopar, H. Kusic, and N. Koprivanac, "Treatment of simulated industrial wastewater by photo-Fenton process. Part I: The optimization of process parameters using design of experiments (DOE)," Chem Eng J., vol. 173, No. 2, pp. 267–279, DOI: 2011, 10.1016/j.cej.2010.09.070.

[3] Y. H. Huang, Y. J. Huang, H. C. Tsai, and H. T. Chen, "Degradation of phenol using low concentration of ferric ions by the photo-Fenton process," J Taiwan Inst Chem Eng., vol. 41, No. 6, pp. 699–704, 2010, DOI: 10.1016/j.jtice.2010.01.012.

[4] S. Q. Liu, L. R. Feng, N. Xu, Z. G. Chen, and X. M. Wang, "Magnetic nickel ferrite as a heterogeneous photo-Fenton catalyst for the degradation of rhodamine B in the presence of oxalic acid," Chem Eng J., vol. 203, pp. 432–439, 2012, DOI: 10.1016/j.cej.2012.07.071.

[5] H. B. Hadjltaief, P. Da Costa, P. Beaunier, M. E. Gálvez, and B. M. Zina, "Fe-clay-plate as a heterogeneous catalyst in photo-Fenton oxidation of phenol as probe molecule for water treatment," Appl Clay Sci., Vol. 91–92, pp. 46–54, 2014, DOI: 10.1016/j.clay.2014.01.020.

[6] C. E. Diaz-Uribe, L. Vallejo and J. Miranda, "Photo-Fenton oxidation of phenol with Fe(III)-tetra-4-carboxyphenylporphyrin/SiO$_2$ assisted with visible light," J. Photochem. Photobiol., A. Vol. 294, pp. 75–80, 2014, DOI: 10.1016/j.jphotochem.2014.08.004.

[7] Z. Mesgari, M. Gharagozlou, A. Khosravi, and K. Gharanjig, "Spectrophotometric studies of visible light induced photocatalytic degradation of methyl orange using phthalocyanine-modified Fe-doped TiO$_2$ nanocrystals," Spectrochim Acta A Mol Biomol Spectrosc, Vol. 92, pp. 148–153, 2012, DOI: 10.1016/j.saa.2012.02.055.

[8] S. Ivanova, A. Penkova, M. Hidalgo, J. A. Navío, F. Romero-Sarria, M. A. Centeno, and J. A. Odriozola, "Synthesis and application of layered titanates in the photocatalytic degradation of phenol," Appl Catal B., Vol. 163, pp. 23–29, 2015, DOI: 10.1016/j.apcatb.2014.07.048.

[9] A. Di-Paola, E. García-López, G. Marcì, C. Martín, L. Palmisano, V. Rives, and A. M. Venezia, "Surface characterisation of metal ions loaded TiO$_2$ photocatalysts: Structure-activity relationship," Appl Catal B., Vol. 48, No. 3, pp. 223–233, 2004, DOI: 10.1016/j.apcatb.2003.10.015.

[10] B. N. Shi, J. F. Wan, C. T. Liu, X. J. Yu, and F. W. Ma, "Synthesis of CoFe$_2$O$_4$/MCM-41/TiO$_2$ composite microspheres and its performance in degradation of phenol," Mat Sci Semicon Proc., Vol. 37, pp. 241–249, 2015, DOI: 10.1016/j.mssp.2015.03.048.

[11] C. Yu, Q. Fan, Y. Xie, J. Chen, Q. Shu, and J. C. Yu, "Sonochemical fabrication of novel square-shaped F doped TiO$_2$ nanocrystals with enhanced performance in photocatalytic degradation of phenol," J Hazard Mater., Vol. 237–238, pp. 38–45, 2012, DOI: 10.1016/j.jhazmat.2012.07.072.

[12] M. Minella, G. Marchetti, E. De Laurentiis, M. Malandrino, V. Maurino, C. Minero, D.Vione, and K. Hanna, "Photo-Fenton oxidation of phenol with magnetite as iron source," Appl Catal B., Vol. 154–155, pp. 102–109, 2014, DOI: 10.1016/j.apcatb.2014.02.006.

[13] D. V. Wellia, Q. C. Xu, M. A. Sk, K. H. Lim, T. M. Lim, and T. T. Tan, "Experimental and theoretical studies of Fe-doped TiO$_2$ films prepared by peroxo sol-gel method,". Appl Catal A. Vol. 401, No. 1–2, pp. 98–105, 2011, DOI: 10.1016/j.apcata.2011.05.003.

[14] X. Feng, H. Guo, K. Patel, H. Zhou, and X. Lou, "High performance, recoverable Fe$_3$O$_4$ZnO nanoparticles for enhanced photocatalytic degradation of phenol," Chem Eng J., Vol. 244, pp. 327–334, 2014, DOI: 10.1016/j.cej.2014.01.075.

[15] H. Ling, K. Kim, Z. Liu, J. Shi, X. Zhu, and J. Huang, "Photocatalytic degradation of phenol in water on as-prepared and surface modified TiO$_2$ nanoparticles," Catal Today, Vol. 258, pp. 96–102, 2015, DOI: 10.1016/j.cattod.2015.03.048.

[16] S. Sohrabi, and F. Akhlaghian, "Modeling and optimization of phenol degradation over copper-doped titanium dioxide photocatalyst using response surface methodology," Process Saf Environ., Vol. 99, pp. 120–128, 2016, DOI: 10.1016/j.psep.2015.10.016.

[17] Y. Zhang, R. Selvaraj, M. Sillanpää, Y. Kim, and C. W. Tai, "The influence of operating parameters on heterogeneous photocatalytic mineralization of phenol over BiPO$_4$," Chem Eng J., Vol. 245, pp. 117–123, 2014, DOI: 10.1016/j.cej.2014.02.028.

[18] R. L. Narayana, M. Matheswaran, A. A. Aziz, and P. Saravanan, "Photocatalytic decolourization of basic green dye by pure and Fe, Co doped TiO$_2$ under daylight illumination," Desalination. Vol. 269, No. 1–3, pp. 249–253, 2011, DOI: 10.1016/j.desal.2010.11.007.

[19] Y. Liu, J. H. Wei, R. Xiong, C. X. Pan, and J. Shi, "Enhanced visible light photocatalytic properties of Fe-doped TiO$_2$ nanorod clusters and monodispersed nanoparticles," Appl Surf Sci., Vol. 257, pp. 8121–8126, 2011, DOI: 10.1016/j.apsusc.2011.04.121.

[20] B. Babić, J. Gulicovski, Z. Dohčević-Mitrović, D. Bučevac, M. Prekajski, J. Zagorac, and B. Matović, "Synthesis and characterization of Fe^{3+} doped titanium dioxide nanopowders," Ceram. Int., Vol. 38, No. 1, pp. 635–640, 2012, DOI: 10.1016/j.ceramint.2011.07.053.

[21] A. Montesinos-Castellanos, and T. A. Zepeda, "High hydrogenation performance of the mesoporous NiMo/Al(Ti, Zr)-HMS catalysts," Micropor. Mesopor. Mat., Vol. 113, No. 1–3, pp. 146–162, 2008, DOI: 10.1016/j.micromeso.2007.11.012.

[22] M. C. Capel-Sanchez, J. M. Campos-Martin, J. L Fierro, M. P. de Frutos, and A. P. Polo, "Effective alkene epoxidation with dilute hydrogen peroxide on amorphous silica-supported titanium catalysts," Chem. Commun. Vol.10, pp. 855–856, 2000, DOI: 10.1039/B000929F.

[23] M. Crisan, D. Mardare, A. Ianculescu, N. Dragan, I. Nitoi, D. Crisan, M. Voicescu, L. Todan, P. Oancea, C. Adomnitei, M. Dobromir, M. Gabrosvska and B. Vasile, "Iron doped TiO$_2$ films and their photoactivity in nitrobenzene removal from water," Appl. Surf. Sci. Vol. 455, pp. 201–215, 2018, DOI: 10.1016/j.apsusc.2018.05.124.

[24] C. Adán, A. Bahamonde, I. Oller, S. Malato, and A. Martínez-Arias, "Influence of iron leaching and oxidizing agent employed

on solar photodegradation of phenol over nanostructured iron-doped titania catalysts," App Catal B. Vol. 144, pp. 269–276, 2014, DOI: 10.1016/j.apcatb.2013.07.027.

[25]   Q. Wu, C. Yang, and R. Krol, "A dopant-mediated recombination mechanism in Fe-doped TiO$_2$ nanoparticles for the photocatalytic decomposition of nitric oxide," Catal Today, Vol.   225,   pp.   96–101,   2014,   DOI: 10.1016/j.cattod.2013.09.026.

Daniela Hurtado J., was born in Itagüi Antioquia, in the year of 1996, she finished her basic studies in 2013, received her title of Technologist in Industrial Chemistry and Laboratory in 2019 at the Politécnico Colombiano Jaime Isaza Cadavid.

https://scienti.colciencias.gov.co/cvlac/visualizador/generarCurriculoCv.do?cod_rh=0000060782

E. Arriola-Villaseñor. Engineer in Energy from Universidad Autónoma Metropilitana (UAM - Iztapalapa), 2012. M.Sc. in Chemical Engineering from the same university, 2015. His research involves the synthesis and catalytic characterization of mono and bimetallic catalysts on basic supports suitable for biomass conversion. He has substantial experience in the field of environmental bioremediation. He has numerous national and international journal publications and has participated in some national and international conferences. Erasmo is Researcher Professor from Politécnico Colombiano Jaime Isaza Cadavid.
https://scienti.colciencias.gov.co/cvlac/visualizador/generarCurriculoCv.do?cod_rh=0000060915

Eliana Berrío M. was born in Medellín in 1994. She is a Technologist in Industrial and Laboratory Chemistry of the Politecnico Jaime Isaza Cadavid (2015), also an Environmental Engineering student at the University of Antioquia (2015-Present). Since 2016 she works as an analyst at the Environmental Laboratory of Water Resource Management (LAGREH), of the Politecnico Jaime Isaza Cadavid, she is also an active member of the CAMER research group - Environmental Catalysis and Energy Renewable. Among the activities she works as an analyst is the establishment and implementation of the quality management system and standardization and verification of methods for water analysis in the LAGREH laboratory.
http://scienti.colciencias.gov.co:8081/cvlac/visualizador/generarCurriculoCv.do?cod_rh=0001513117

Jose A. Hernandez Maldonado. was born in Mexico City in 1977. He is Chemical engineer graduated from the Universidad Autonoma Metropolitana-Iztapalapa (2004). Master in chemical sciences (2006) and PhD Chemistry 82012) in the same university. Since 2009 he has been a professor (currently in the ranks: Associate B) of the Department of Integral and Institutional Academic Training of Unidad Profesional Interdisciplinaria de Ingeniería Campus Guanajuato - Instituto Politécnico Nacional. In teaching, the performance focuses on the areas of Transport phenomena, Fluid - Fluid Bioseparations, Bioseprations Laboratory at an undergraduate level. In research the areas of interest focus on bioremediation using agroindustrial waste, biocatalysis using immobilized enzymes, obtaining biomaterials for the use of new excipients for medications and for bone regeneration. He has authored numerous scientific publications in indexed journals and since 2016 he is a member of the national system of researchers (SNI) of CONACYT.

Trino A. Zepeda was born in Michoacán, Mexico in 1979. He is a Chemical Engineer, from the University of Colima. He completed his master's and doctoral studies in Chemical Engineering at the Faculty of Chemistry of the Autonomous University of Mexico, has made research stays in several national and international prestige laboratories. Since 2010, he joined the Center for Nanosciences and Nanotechnology at UNAM-Ensenada, where he is currently a senior researcher "B". His research work focuses on the study of nanocatalysts for obtaining of ultra-clean fuels. Within this research line: it has contributed to the production of ultra-low sulfur diesel and gasoline, both in basic science studies and in technological developments. In parallel, it studies and develops catalysts for the synthesis of light synthetic hydrocarbons (C1-C$_4$ fraction) and of medium molecular weight (gasolines type fraction C$_5$-C$_9$) via Fischer Tropsch process. Additionally it contributes in obtaining hydrogen via reforming of light hydrocarbons and via water-gas shift reaction.
https://www.cnyn.unam.mx/index.php?option=com_perfil&view=perfil&Itemid=56&uid=138&lang=en

Gina Marcela Hincapié Triviño was born in 1984 in Pereira. She studied Chemistry Technology at Universidad Tecnológica de Pereira (2005), Chemistry at Universidad de Antioquia (2009) and Ph.D in Chemistry Sciences (2014) at the same University. Since 2018 she is working as Professor at Chemistry Department of Sciences Faculty at Universidad Nacional de Colombia Sede Bogotá and researcher in Solid State and Environmental Catalysis group. Her teaching areas are focused on Analytical Chemistry, specially treating instrumental analysis. Her research is focused on heterogeneous catalysis. She aims to gain

an elemental understanding of active sites on the surface of catalysts to explain the behavior of chemical reactions and to develop new catalysts.

http://scienti.colciencias.gov.co:8081/cvlac/visualizador/generarCurriculoCv.do?cod_rh=0000974048

Rolando Barrera-Zapata was born in Medellín in 1974. He is a chemical engineer graduated from the University of Antioquia (2003). Master in chemical sciences (2007) and Doctor in engineering (2010) from the same University. Since 2012 he has been a professor (currently in the ranks: associate) of the Department of Chemical Engineering of the Faculty of Engineering of the University of Antioquia and since 2014 he is also coordinator of the CERES Research Group - Agroindustry & Engineering. In teaching (both undergraduate and graduate), he focuses on the areas of chemical reaction engineering, numerical methods in applied mathematics and process simulation, . In research the areas of interest focus on modeling, simulation and process optimization; agroindustrial processes; extraction and valuation of natural products; thermochemical biorefineries, catalysis and kinetics of chemical reactions. He has authored several university text-books, numerous scientific publications in indexed journals and simulation software.

http://scienti.colciencias.gov.co:8081/cvlac/visualizador/generarCurriculoCv.do?cod_rh=0000147729

Alba N. Ardila Arias is PhD in Chemical Engineering from Universidad Autónoma Metropilitana (UAM - Iztapalapa), 2017. M.Sc. in Chemistry Sciences from Universidad de Antioquia, 2008. Specialist in Science Education with Emphasis in Mathematics and Physics, Universidad Pontificia Bolivariana, 2004. Specialist in Water Management, Universidad de Antioquia, 2010. Her research involves the synthesis and catalytic characterization of mono and bimetallic catalysts on basic supports suitable for biomass conversion. Her scientific interests are in the areas of nanotechnology and material science, biomass conversion, catalysis and photocatalysis. She has substantial experience in the field of analytical techniques, including analysis methods and equipment. She has received different awards and scholarships. She has also been awarded with different academic honors and prizes. She has numerous national and international journal publications and has participated in many national and international conferences. Alba is Researcher and Associate Professor at Politécnico Colombiano Jaime Isaza Cadavid.

http://scienti.colciencias.gov.co:8081/cvlac/visualizador/generarCurriculoCv.do?cod_rh=0000469815